Atmospheric Research 135–136 (2014) 102–111

Contents lists available at ScienceDirect

Atmospheric Research

journal homepage: www.elsevier.com/locate/atmos

The effect of aerosols on long wave radiation and global warming

Y. Zhou *, H. Savijärvi

Department of Physics, Division of Atmospheric Sciences, University of Helsinki, P.O. Box 14, FI-00014, Finland

ARTICLE INFO

Article history:
Received 21 January 2013
Received in revised form 18 August 2013
Accepted 20 August 2013

Keywords:
Aerosols
Long wave radiation
Radiative forcing
Long wave heating rate

ABSTRACT

The effect of aerosols on long wave (LW) radiation was studied based on narrowband LW calculations in a reference mid-latitude summer atmosphere with and without aerosols. Aerosols were added to the narrowband LW scheme based on their typical schematic observed spectral and vertical behaviour over European land areas. This was found to agree also with the spectral aerosol data from the Lan Zhou University Semi-Arid Climate Observatory and Laboratory measurement stations in the north-western China.

A volcanic stratospheric aerosol load was found to induce local LW warming and a stronger column "greenhouse effect" than a doubled CO_2 concentration. A heavy near-surface aerosol load was found to increase the downwelling LW radiation to the surface and to reduce the outgoing LW radiation, acting very much like a thin low cloud in increasing the LW greenhouse effect of the atmosphere. The short wave reflection of white aerosol has, however, stronger impact in general, but the aerosol LW greenhouse effect is non-negligible under heavy aerosol loads.

1. Introduction

The earth is in a near radiation balance, the outgoing long wave (thermal) radiation (OLR) closely balancing the absorbed solar radiation. The effect of clouds on OLR and on the cloud radiative forcing (CRF), can be estimated from satellite data by taking the difference between the clear sky scenes and all scenes. These observations indicate that clouds increase the planetary shortwave (SW) albedo by 15% to 30%, thereby reducing the absorbed solar radiation by about 50 W/m^2. This cooling effect is opposed by the warming effect of clouds on the longwave (LW) radiation (the "cloud LW greenhouse" effect), which reduces the OLR by about 31 W/m^2 (Hartmann, 1994) on the average.

This study concentrates on the analogous long wave radiative effect ("LW forcing") caused by airborne aerosols (other than clouds), which is less well-known than that of the clouds. During the 1970s, the influence of the aerosol layer height and the changes of surface albedo on the atmospheric radiation balance were investigated by Reck (1974, 1975). The results of those pioneering studies showed that like the clouds, aerosols produce two opposing effects in the atmosphere: they cause heating of the Earth's surface by enhancing the downwelling LW radiation, but they also increase the planetary SW albedo, which causes a cooling effect. The combined effect depends on many factors including the aerosol type, concentration and height. It also varies on time due to the diurnal and seasonal changes in incoming solar radiation. The cooling effect due to a reduction of the incoming solar radiation often dominates at daytime while the weaker warming effect due to the aerosol LW emission is present throughout the day and may be observed at night time.

In the 1980s, new methods were developed for investigating the aerosol characteristics and their effects on the albedo and climate. These include for example the multi-wavelength satellite extinction measurements (Lenoble, 1986), and balloon or aircraft measurements. At the same time the focus also turned towards the effects of volcanic

* Corresponding author at: University of Helsinki, P.O. Box 14, FI-00014, Finland. Tel.: +358 465646403.
E-mail addresses: zy791@hotmail.com, yxzhou@mappi.helsinki.fi (Y. Zhou).

0169-8095/$ – see front matter © 2013 Elsevier B.V. All rights reserved.
http://dx.doi.org/10.1016/j.atmosres.2013.08.009

aerosol loads in the stratosphere as well as to the effects of aerosols on the local climate in specific locations. The latter was investigated for example in the city of St. Louis, USA in (Method and Carlson, 1982). These studies showed that the effects of aerosols are similar to those of a thin cloud at the same height. The impact is small in magnitude, however and somewhat difficult to measure unless the aerosol concentration is extremely high. The 1990s saw significant increase of research on aerosols and their effect on climate. First computer models of the effects of aerosols on the radiation balance were developed. One such model is presented by Claquin et al. in (Claquin et al., 1997).

In the 21st century, the work of studying and understanding the effects of both natural and anthropologic aerosols on the radiation balance both globally (Dammann et al., 2000) and locally (Shaocai et al., 2001; Han et al., 2012) has continued. The effects of specific types of aerosols or effects of aerosols in specific locations have also been studied (Verma et al., 2006; Wendisch et al., 2008). Most recently, the radiative effects of aerosols have been studied in both urban and remote areas of western India in 2011 (Ramachandran and Kedia, 2011), and Europe (Péré et al., 2012), USA (Mickley et al., 2012) and China (Zhang et al., 2012) in 2012. The results show significant variability of the radiative effects due to the meteorological conditions as well as the aerosol loads themselves. Therefore the aerosol processes and meteorological processes appear to be coupled and they interact with each other. This is best studied by using atmospheric and radiative models equipped with aerosol schemes and using aircraft and satellite measurements. In this way, for instance, the major Saharan dust storms have been shown to imply considerable differences into the surface LW fluxes and OLR (Haywood et al., 2005; Slingo et al., 2006; Hansell et al., 2010). However, such coupled studies, although the most complete, are dominated by the strong daytime SW effects of dust, and so may not be optimal in isolating and characterizing the LW effects and mechanisms.

In this study the OLR differences, the LW surface budget differences and the internal LW heating/cooling rates are studied by comprehensive narrowband LW model calculations, using various aerosol loads in typical mid-latitude conditions. In particular, the observed aerosol loads of north-western China are used as an extreme example, because the wind-blown mineral dust from the surrounding deserts and the heavy industrial pollution in the city of Lan Zhou provide quite large natural and anthropologic aerosol loads for this region. This was analyzed by making LW calculations in a typical mid-latitude summer air column (MLS case) (Ellingson et al., 1991) with a narrow-band spectral LW scheme (Savijärvi, 2006), while introducing variable aerosol, cloud, and greenhouse gas loads into the scheme. The results for the different cases were compared. In particular the aerosol effects on the OLR, on the down-welling LW radiation at the surface (DLR), and on the internal LW heating rate in the atmosphere (LH) with different aerosol and greenhouse gas loads was analyzed.

2. Methodology

2.1. The long-wave radiation scheme

Long wave radiation in the Earth's atmosphere is defined as the electromagnetic radiation at wavelengths longer than 4 μm, usually from terrestrial origin. The short wave (SW) radiation wavelengths are less than 4 μm. It is usually from solar origin. The thermal LW and solar short wave radiation propagate in the atmosphere, experiencing absorption, emission, scattering and reflection. Unbalanced radiation will lead to variations in the atmospheric, ground and ocean temperatures and air movements (i.e. winds, weather and climate).

The ground and ocean are the main direct heat sources for the troposphere. They absorb solar radiation, for which the atmosphere is relatively transparent. The water vapour, CO_2 and other types of greenhouse gases in the atmosphere have varying abilities to absorb and emit LW radiation. Therefore the LW radiation emitted by the sun-heated ground will propagate through the atmosphere back to space only in the spectral LW window(s) of the greenhouse gases, since O_2 and N_2 are transparent to LW radiation. In general, 75% to 95% of the LW emission of the ground is absorbed by the water vapour, CO_2, O_3 and other greenhouse gases in the troposphere, and re-emitted at the air temperatures to all directions, hence partially back to the ground, creating the "greenhouse effect". How aerosols then impact this LW greenhouse effect is the subject of this study.

The LW radiation scheme (taken from (Savijärvi, 2006)) calculates the upwelling and downwelling LW fluxes (F_{up}, F_{down}) at each altitude from solutions to the plane-parallel equation of radiative transfer, using the absorption (nonscattering) approximation with a diffusivity factor of 1.66, and assuming local thermodynamic equilibrium. The spectral fluxes at each wave number $k = 1/\lambda$ for a narrow band Δk around k were calculated with a statistical narrow-band model (NBM) for the gaseous transmissivity $t_{gas,k}$ at each band. The NBM covers the 0–1200 cm^{-1} wave number range in 48 bands ($\Delta k = 25\ cm^{-1}$), the 1200–2100 cm^{-1} range in 18 bands ($\Delta k = 50\ cm^{-1}$), and the 2100–2500 cm^{-1} range in one band; so there are 67 bands in the LW range. The band parameters for water vapour, CO_2 and O_3 were taken from (Houghton, 2002). The Goody random band model was adopted for water vapour, the Malkmus model for CO_2 and O_3, and the Curtis-Godson method was used for line pressure broadening along inhomogeneous vertical paths. The Roberts *et al.* scheme (1976) (Roberts et al., 1976), augmented with foreign-broadened contribution, was used for the important water-vapour continuum effect in this study, where we concentrate on the boundary layer, although we recommend the more comprehensive Clough et al. (1992) continuum scheme (Clough et al., 1992) for studies that would concentrate on the upper troposphere.

The local LW heating rate of air is obtained as the vertical convergence of the total net LW flux $F_{net} = F_{up} - F_{down}$. Thus at each height z, LH is given by:

$$LH(z) = \left(\frac{\partial T}{\partial t}(z)\right)_{LWR} = -\frac{1}{\rho C_p}\frac{\partial}{\partial z}\left(F_{up} - F_{down}\right) = \frac{g}{C_p}\frac{\partial F_{net}}{\partial p} \quad (1)$$

Here ρ is the density of air and C_p the specific heat of air at constant pressure p. The last form follows from the hydrostatic relation.

The NBM should be validated before using it for aerosol-laden atmospheres. This was made in (Savijärvi, 2006), where the key LW flux values were compared with results from the International Comparison of Radiation Codes in Climate Models

(ICRCCM) for the mean mid-latitude summer (MLS) input profiles for temperature, water vapor and O_3 (Ellingson et al., 1991), and also with values obtained using the Clough et al. (1992) water-vapour LBL model (Clough et al., 1992) with their continuum. These comparisons showed that the present NBM was within the narrow range of the LBL results, and is very close to the 35-model all-gases median of the comparison. Thus the clean and clear sky reference MLS case is well simulated by the present NBM.

2.2. Aerosols in the LW Scheme

The atmospheric aerosols may influence the climate in three ways: Firstly, aerosol particles absorb and scatter solar radiation and change the SW energy budget of the Earth–atmosphere system. Secondly, aerosol particles form cloud condensation nucleii (CCN), and thus act on the optical properties, distribution and life cycle of clouds. Finally, the aerosols also influence the thermal radiation field around the Earth by affecting DLR, OLR and LH. This last effect is the least known of the three effects and it is studied in this work.

Aerosols were added to the above spectral NBM scheme by assuming their typical schematic observed behaviour over European inland areas (Paltridge and Platt, 1976). The aerosol volume extinction coefficient β_{ae} (km^{-1}) is hence set to

$$\beta_{ae} = 0.2\,km^{-1}\left(\frac{20\,km}{V}\right)\left(\frac{0.55\,\mu m}{\lambda}\right)e^{-\left(\frac{z}{H}\right)} \quad (2)$$

The aerosol concentration is assumed to decay upward exponentially with a scale height H (~1 km). At the surface β_{ae} is 0.2 km^{-1} at the reference visible wavelength $\lambda = 0.55$ μm, when the horizontal meteorological visibility V is 20 km, and it is assumed to be inversely proportional to both V and λ. These assumptions were verified with many careful spectral aircraft and tower observation campaigns of aerosols made around the north western China and in the city of Lan Zhou (Wu, 1998; Zhao et al., 2005; Deng et al., 2010). The observations were made at and around the Semi-Arid Climate Observatory and Laboratory (SACOL) stations of the University of Lan Zhou.

The aerosol vertical optical depth (AOD; τ) is calculated as

$$\tau = \int \beta_{ae}(z)dz \quad (3)$$

for each layer and each wavelength band in the NBM. Assuming no scattering (a good approximation in the LW range) the LW diffuse transmissivity of aerosols is

$$t_a = e^{-1.66\tau} \quad (4)$$

and the total transmissivity is $t = t_{gas} \cdot t_a$ for each layer and each band. Thus the aerosols are ineffective in the opaque bands, where t_{gas} ~ 0, and have their biggest impact in the LW window(s), where t_{gas} ~ 1.

The near surface values of β_{ae} at $\lambda = 9$–10 μm within the LW window region are about 0.01 km^{-1} from Eq. (2) during the typical visibility of 20 km. This agrees with other continental LW aerosol models and LW observations from the literature (See e.g. Table 9.2 and Fig 9.9 in (Paltridge and Platt, 1976)).

3. Results

3.1. Reference case: clear sky MLS with 300 ppm of CO_2

The clear sky mean mid-latitude summer (MLS) case of the Intercomparison of Radiation Codes in Climate Models, with 300 ppm of CO_2 and no aerosols/clouds was used as the reference case. The main MLS input variables are T(z) and q(z), where T is the temperature and q the water vapour mixing ratio. The temperature profile is shown graphically in Fig. 1. The ozone profile and q(z) are given by Ellingson et al. in (Ellingson et al., 1991). The LW scheme output, i.e. the downward and upward fluxes, the net flux (all in W m^{-2}), and the LW heating rate (K day^{-1}) (Eq. (1)), are shown in Figs. 2 and 3.

At the model top (104 km), the OLR is 287.57 W m^{-2} and the downward LW flux is assumed to be zero. At the surface the DLR is 344.76 W m^{-2} and the upward flux is 423.62 W m^{-2}. The ground emissivity is assumed to be 1, which corresponds to the blackbody emission, σT^4, of the surface (at 294 K). The net flux difference is therefore 78.85 W m^{-2} at the surface. The net flux increases upward (Fig. 2), its gradient giving the local LW heating rate (Eq. (1)). It is about −3.8 K day^{-1} near the surface and about −2 K day^{-1} in the upper troposphere, as shown in Fig. 3.

3.2. An extreme case: aerosol particle pollution in north-western China and Lan Zhou city

The city of Lan Zhou (36º02′ N, 103º48′ E) has the worst air quality among all the cities in China. It is among the 30 most polluted cities in the world. The map in Fig. 4 shows the location of Lan Zhou in China. It is close to the north-western desert areas, from where the winds often bring in mineral dust aerosol. The population of about 1 million and heavy industry also produce a large anthropologic aerosol load locally. The city is located in the Yellow River canyon, which makes it a “smog trap” (Savijärvi and Jin, 2001). During a sand storm, the minimum horizontal visibility V in Lan Zhou can be as low as 300 m.

The observed mean concentration of some aerosol particles in Lan Zhou city between the years 2005 and 2008 has been: SO_2: 0.0610 mg m^{-3}, NOx: 0.066 mg m^{-3}, PM_{10}: 0.431 mg m^{-3} and PM2.5: 0.276 mg m^{-3}. The recommended daily limits for PM_{10} and $PM_{2.5}$ by the European Union are 0.05 mg m^{-3} and 0.04 mg m^{-3} respectively. The annual limits are 0.03 mg m^{-3} and 0.02 mg m^{-3}. The daily $PM_{2.5}$ concentration should not exceed the annual limit more than 14 times per year. The daily and annual PM_{10} limits in Sweden are 0.10 mg m^{-3} and 0.02 mg m^{-3} respectively. The observed mean PM_{10} and $PM_{2.5}$ concentrations in Lan Zhou in 2005–2008 were therefore more than ten times the allowed annual limits in EU and Sweden.

The SACOL observations of aerosols around and in Lan Zhou, along with observations in Europe, were used to create and validate the detailed aerosol model used in the NBM scheme (Eq. (2)) (Wu, 1998; Zhao et al., 2005; Deng et al., 2010). The values of the key LW quantities, DLR, OLR and LH,

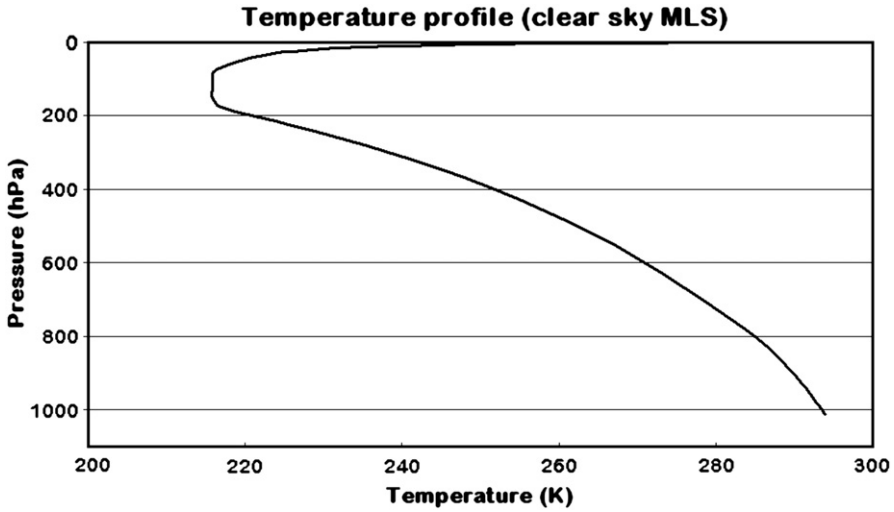

Fig. 1. The MLS temperature profile used as an input variable for the LW scheme.

in conditions similar to those in Lan Zhou are shown in the tables of Section 3.3. The extreme case $V = 0.3$ km in Table 4 resembles the observed conditions during a typical sand-storm. These aerosol observations were used for model validation because they include both polluted urban and continental desert aerosol cases, they are carefully made, and they include some of the heaviest aerosol loads observed in the northern hemisphere.

3.3. Effect of aerosols on LW fluxes

The NBM model was applied to the reference MLS data with different profiles for clouds, CO_2 and aerosols in order to better understand the factors changing the key LW quantities (DLR, OLR and LH).

The cloud radiative forcing (CRF) was first studied to give a background by varying the cloud liquid water vertical path (LWP) in the NBM model. The CRF estimated from satellite measurements is shown as a reference in Table 1 from (Hartmann, 1994). The NBM model results are listed in Table 2.

From Table 2, one can see that a thick low cloud will lead to a strong increase in the DLR and to a decrease in the OLR, the latter in agreement with the satellite measurements (satellites cannot measure the DLR change below clouds). Further, the thick low cloud will also lead to the increase of the column longwave cooling rate. At 100 g m^{-2} the cloud has reached a blackbody state and so any larger LWP (e.g. 300 g m^{-2}) produces no further change.

The effect of the CO_2 concentration on the LW quantities was also studied. According to the NBM model applied on the MLS case, the increase of the CO_2 concentration from

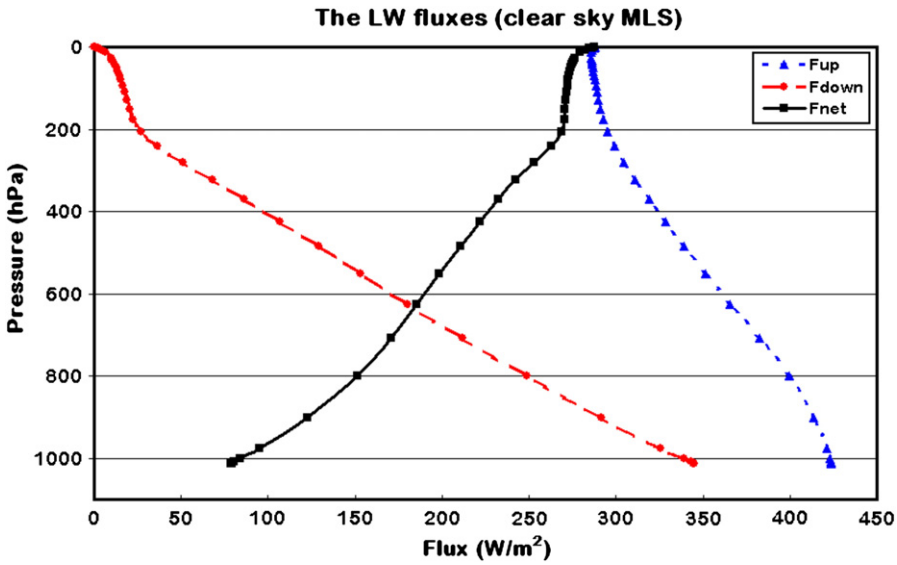

Fig. 2. The LW fluxes in the clear sky MLS case without aerosol.

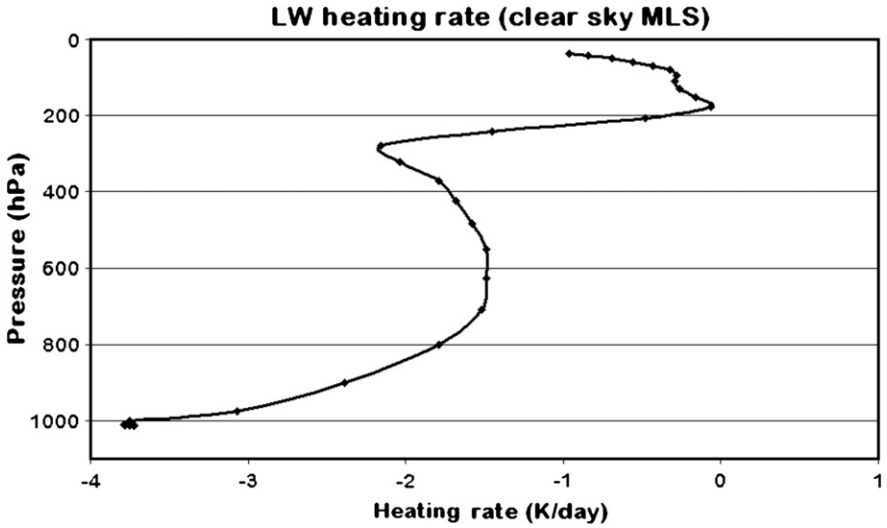

Fig. 3. The local LW heating rate in the clear sky MLS case without aerosol.

300 ppm to 600 ppm increases the DLR by about 2 W m^{-2}, while the OLR decreases by about 2.2 W m^{-2}. This results in a minor increase of the LH from −1.739 K/day to −1.737 K/day. These values are in good agreement with the estimated global mean radiative forcing of doubled CO_2.

The NBM model was first applied to modelling the effects of aerosols on the LW quantities by studying the influence of a heavy aerosol load in the stratosphere. An aerosol layer with constant $\beta_{ae} = 0.1$ km^{-1} at 0.55 μm was added to the MLS case between 14 and 24 km. The vertical visible optical depth of this layer was 1. Such an aerosol load could be produced for example by a major volcanic eruption. The results show that a heavy volcanic aerosol load in the stratosphere will increase the DLR slightly, and decrease the OLR moderately. The DLR increase was 1.71 W m^{-2} and the OLR decrease 20.58 W m^{-2}. As the volcanic dust layer net absorbs the surface emission, there is also a temporary 0.157 K/day decrease in the LW cooling rate.

Tropospheric aerosols were modelled using two different approaches, and the results were compared. The first assumes a vertically constant low-level aerosol volume extinction coefficient β_{ae} (km^{-1}) and the second approach assumes an exponentially decaying aerosol load (Eq. (2)). The NBM results with constant β_{ae} are listed in Table 3.

The results in Table 3 show that a vertically constant dust layer with $\tau > 0.2$ increases the DLR more than the doubled CO_2 did. On the other hand the near-surface dust load has a lesser effect on the outgoing long-wave radiation at the top of the atmosphere than the doubled CO_2 concentration. Assumption of constant β_{ae} with height is, however, usually less realistic than the exponentially decaying dust load (Deng et al., 2010). Table 4 therefore shows results for the exponentially decaying aerosol model (Eq. (2)) with the aerosol scale height H = 1 km, as the function of visibility.

The results listed in Table 4 show that the typical "good visibility" of $V = 20$ km ($\tau_{vis} \sim 0.2$) corresponds to the DLR increase of 2.24 W m^{-2} and the OLR decrease of only 0.23 W m^{-2} from the clear sky reference case. The DLR increases of Table 4 are similar to those reported in (Hansell et al., 2010) for Saharan dust. The values of the LW quantities obtained with the two different approaches for the same τ_{vis} agree quite well. The lowest row, an extreme case of a really low visibility, $V =$ 300 m, represents conditions during a heavy dust storm. It produces $\tau_{vis} \sim 13$. The effect of such a dense dust load is similar to that of a thick low cloud (Table 2), with the DLR increase from the clear sky case being 62 W m^{-2} and the OLR decrease, 10 W m^{-2}.

The relationship between the visibility and the LW quantities was further investigated by varying the scale height H in Eq. (2). The visibility was fixed to V = 20 km. The results are shown in Table 5.

The results of Table 5 show that the increase of the scale height H from 500 m to 2 km increases the AOD from $\tau_{vis} =$ 0.1 to $\tau_{vis} = 0.4$, increases the DLR by 2.62 W m^{-2} and decreases the OLR by 1.01 W m^{-2}. This results in the LW cooling decrease from −1.749 K/day to −1.763 K/day. The visibility $V = 4$ km and the scale height H = 800 m resemble the observed conditions in the city of Lan Zhou and other areas during heavy anthropologic aerosol loads. The corresponding AOD is $\tau_{vis} = 0.85$. According to the NBM model, in such conditions the DLR is 353.55 W m^{-2} and OLR is 286.87 W m^{-2}. This decreases the LH to −1.807 K/day. Comparison of these values with those of Table 2 shows that the impact of the heavy anthropologic aerosol load on the LW quantities is similar to that of a thin low cloud with a LWP of about 1 g m^{-2}.

The combined effects of aerosols and low clouds were investigated by adding an aerosol layer (0–1 km) with constant β_{ae} under a thin low cloud at 1–2 km. The LW quantities with different values of β_{ae} are shown in Table 6.

The values of Table 6 show that a thick aerosol layer below a thin low cloud layer results in a moderate increase of DLR and the longwave cooling rate, but only a small decrease of OLR.

The effect of an aerosol layer on the local LW fluxes and the local LW heating rate was also investigated. Constant

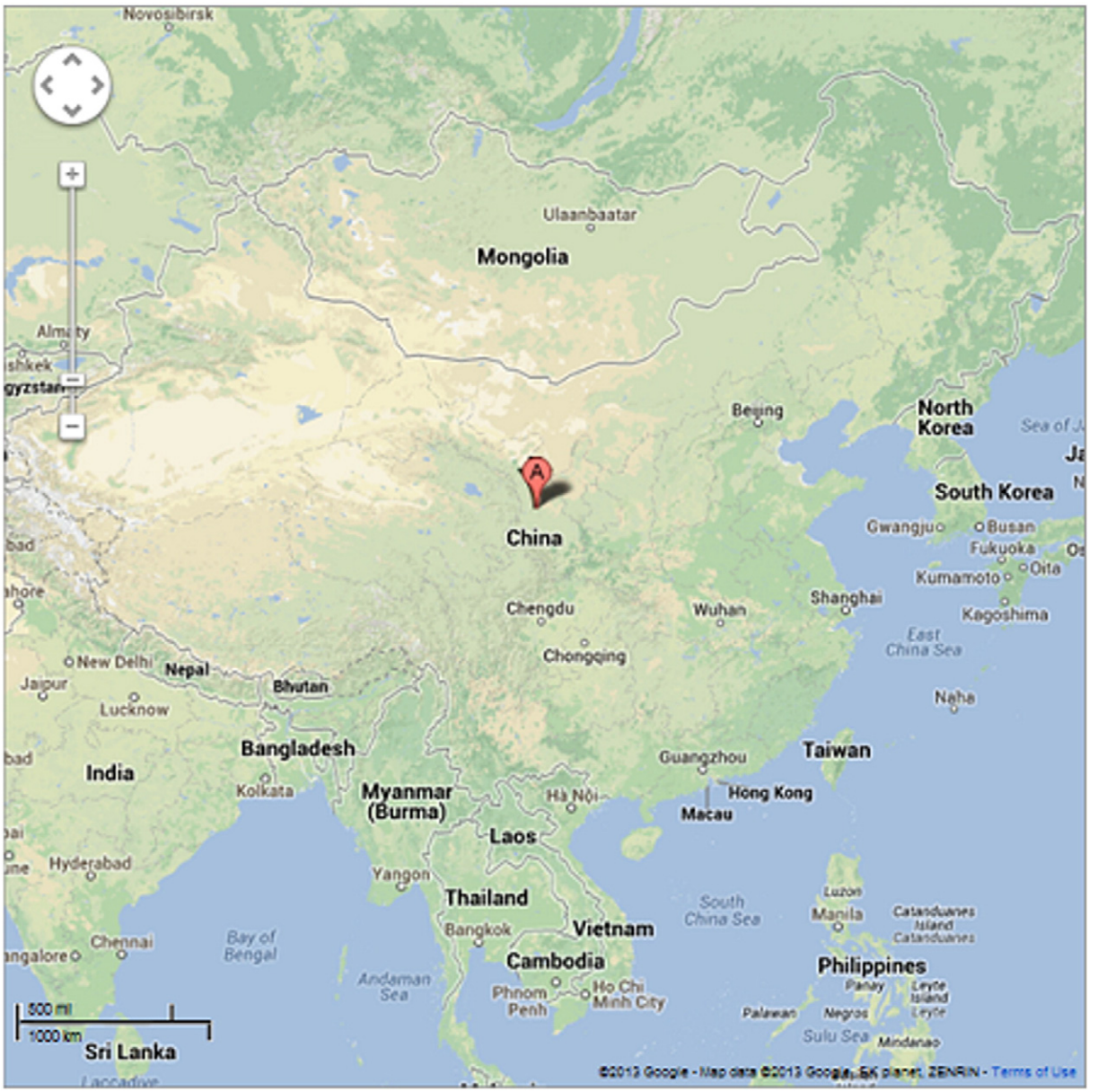

Fig. 4. A Google Maps image showing the location of Lan Zhou city in China.

$\beta_{ae} = 0.1\ \mathrm{km}^{-1}$ at 0.55 μm was used for the near surface aerosol cases. The clear sky MLS case with 300 ppm of CO_2 was used as a reference, and only the deviations from it are shown.

The effect of aerosols to the LW fluxes in the MLS air column is shown in Fig. 5, which displays the LW net flux deviations from the clear sky reference case values (Fig. 2) as

Table 1
Cloud radiative forcing as estimated from satellite measurements (W m^{-2}) (Hartmann, 1994).

	Average	Cloud free	Cloud forcing
OLR	234	266	31
Absorbed solar radiation	239	288	−48
Net radiation	5	22	−17
Albedo	30%	15%	15%

Table 2
The relationship between low cloud thickness (LWP) and the key LW quantities.

Low cloud (1–2 km) LWP g/m^2	DLR W/m^2	OLR W/m^2	LH K/day
0	344.76	287.57	−1.739
1	353.51	286.38	−1.802
10	393.53	280.93	−2.091
100	407.53	279.03	−2.191
300	407.53	279.03	−2.191

Table 3
LW quantities with aerosol layers of different height assuming a vertically constant low-level aerosol volume extinction coefficient $\beta_{ae} = 0.1$ km^{-1} at 0.55 μm.

Aerosol height km	τ_{vis}	DLR W/m^2	OLR W/m^2	LH K/day
0	0	344.76	287.57	−1.739
0–1	0.15	346.41	287.47	−1.752
0–2	0.25	347.35	287.25	−1.758
0–3	0.35	348.17	286.87	−1.762

a function of pressure vertical coordinate. The net flux gradient yields the local LW heating rate by Eq. (1). The variations of the local LW heating rate from the clear sky case are shown in Fig. 6.

Fig. 5 shows that the aerosols act to decrease the net flux from the clear sky value near the top of the current aerosol layer, mainly because F_{down} here increases downward due to the extra LW emission by the aerosol particles, analogously to a thin cloud. This induces LW cooling locally (Fig. 6, Eq. (1)), again as is observed within a thin low cloud. With fixed β_{ae}, the strength of the effect depends on the thickness of the layer, and for a thick layer the decrease gets smaller near the surface. Fig. 6 shows that the clear-sky LW heating rate decreases within the aerosol layer, and the strength of the decrease depends on the thickness of the layer. This local cooling by aerosols is strongest in the middle of each aerosol layer. The LW heating rates above the top of the aerosol layer and near the surface are affected only slightly. An aerosol layer of less than 0–2 km appears to have a small cooling effect very near the surface, while a thicker layer displays a slight warming effect.

Fig. 7 shows how an exponentially decaying aerosol load affects the net LW flux of the MLS air column. The β_{ae} was calculated from the horizontal meteorological visibility V by Eq. (2). Scale height H was set to 1 km. The corresponding LW heating rates are given by Eq. (1). The deviations of the LW heating rate from the clear sky MLS case are shown in Fig. 8.

Comparing Figs. 5–8 and Tables 3 and 4, one can see that the results obtained assuming constant β_{ae} and an exponentially decaying aerosol are slightly different. The effect of exponentially decaying aerosol load on the net flux does not decrease near the surface (as was the case with constant β_{ae}), unless the aerosol concentration is extremely high. As a consequence, the LW cooling effect is always strongest near the surface for light to moderate exponentially upward decaying aerosol loads. The aerosol concentration must be extremely high for it to have a warming effect very near the surface.

Table 4
The relationship between the horizontal meteorological visibility V and the LW quantities for the aerosol LW model (Eq. (2)).

V km	τ_{vis}	DLR W/m^2	OLR W/m^2	LH K/day
∞	0	344.76	287.57	−1.739
50	0.08	345.67	287.48	−1.746
20	0.20	347.00	287.34	−1.756
10	0.40	349.15	287.11	−1.772
1	4.00	377.97	283.53	−1.982
0.3	13.33	406.87	277.26	−2.171

Table 5
The relationship between the visibility, scale height H and the LW quantities for the aerosol LW model (Eq. (2)).

H m	V km	τ_{vis}	DLR W/m^2	OLR W/m^2	LH K/day
500	20	0.11	346.02	287.52	−1.749
800	20	0.17	346.62	287.43	−1.754
1000	20	0.21	347.00	287.34	−1.756
2000	20	0.41	348.64	286.51	−1.763
800	4	0.85	353.55	286.87	−1.807

4. Conclusion

The effect of aerosols on the LW radiation was studied with a LW radiation scheme using a narrowband model for the gaseous absorption and emission of radiation. Aerosols were added to this model by assuming their typical properties according to observations in Europe and in north-western China (Eq. (2)). The ICRCCM mid-latitude summer atmosphere with 300 ppmv of CO_2 was used as a reference case. The impact of aerosols was then studied by adding or varying the amounts of low cloud, CO_2 and aerosols in the MLS case. The heavy natural and anthropologic aerosol loads observed in the city of Lan Zhou in China were used as an extreme example.

The results confirm the hypothesis that an aerosol layer has a similar effect on the LW quantities as a thin cloud, absorbing LW radiation and re-emitting it partially back towards the ground. The result is an increase of the DLR and a slight decrease of OLR. Comparing Tables 2–6, it can be seen that adding a low cloud or tropospheric near-surface aerosol will lead to an increased overall LW cooling rate. However, adding CO_2 or stratospheric aerosol decreases the column LW cooling rate.

The local effect of aerosols was studied by comparing the local net LW fluxes and the local heating rates of the aerosol cases to those of the clear sky reference case. The results show that the LW cooling rate increases from the clear sky case within the near-surface aerosol layer and the strength of the effect depends on the thickness (height) of a fixed well-mixed aerosol layer. The cooling effect is strongest in the middle of the layer and weaker at its top and near the surface. The cooling at the bottom of a shallow aerosol layer is slightly stronger than in the clear sky case, while a high near-surface aerosol layer can lead to a warming effect very near the surface, like a thin cloud or fog. A stratospheric aerosol layer leads on the other hand to local LW warming, again like a thin high cloud layer.

The strength of the effect of aerosols depends also on the aerosol concentration, which is usually highest very near the

Table 6
The LW quantities with a thin low cloud (LWP = 1 g m^{-2}) at 1–2 km and aerosol layer with constant β_{ae} set below it at 0–1 km.

Aerosol amount at 0–1 km β_{ae}, km^{-1}	DLR W/m^2	OLR W/m^2	LH K/day
0	353.51	286.38	−1.802
0.001	353.52	286.38	−1.802
0.01	353.65	286.37	−1.803
0.1	354.94	286.29	−1.814
0.3	357.71	286.11	−1.835
1	366.39	285.52	−1.903

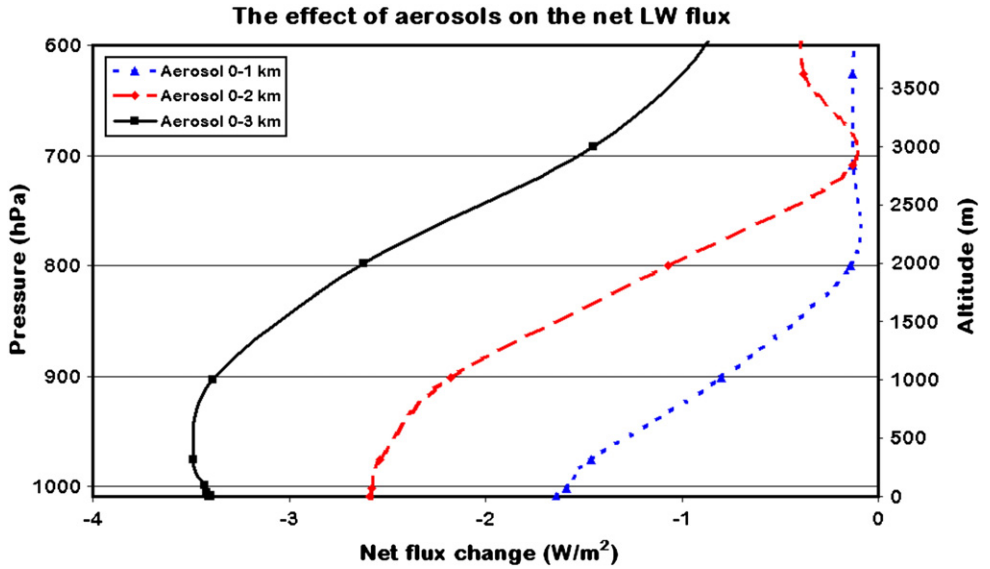

Fig. 5. The effect of aerosols on the net LW flux of the MLS case. Vertically constant β_{ae} of 0.1 km^{-1} at 0.55 μm.

surface. Therefore the LW cooling effect is usually stronger near the surface than near the top of the layer, where the aerosol concentration is lower. In practice, for near-surface aerosols to cause local LW warming at the surface, the concentration has to be extremely high, sand storm-like.

The life assessment studies of the aerosols and greenhouse gases show that lifetimes of tropospheric aerosols range from a few days to a few weeks, depending on their composition, distribution and concentration as well as the altitude and weather conditions (Li and Fan, 2006). The particles with diameter between 0.1 and 10 μm tend to have the longest lifetimes. The radiative forcing effects of the short lived urban and continental aerosols stay mostly near the emission sources, so they essentially affect only the northern hemisphere. On the other hand, the lifetime of greenhouse gas molecules is tens or hundreds of years, and they influence the whole atmosphere.

Atmospheric aerosols influence the solar radiation during the daytime, so their shortwave impact is greatest on low latitudes and during summer. In contrast, the greenhouse gases and aerosols affect the thermal radiation both in daytime and night time. They have influence also during winter and in the middle and high latitudes. The effect of the aerosol particles on SW radiation also depends significantly on the optical properties of the underlying surface reflecting the sunshine. The impact of greenhouse gases is not affected by those. Aerosols also act as CCN, and they can thereby influence the climate indirectly through the changes in the

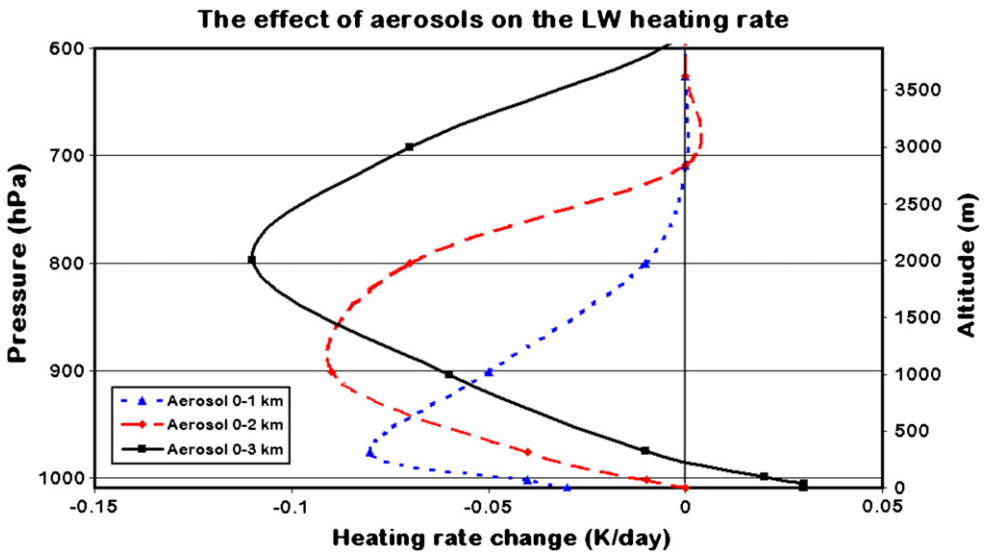

Fig. 6. The effect of aerosols on the LW heating rate of the MLS case. Vertically constant β_{ae} of 0.1 km^{-1} at 0.55 μm.

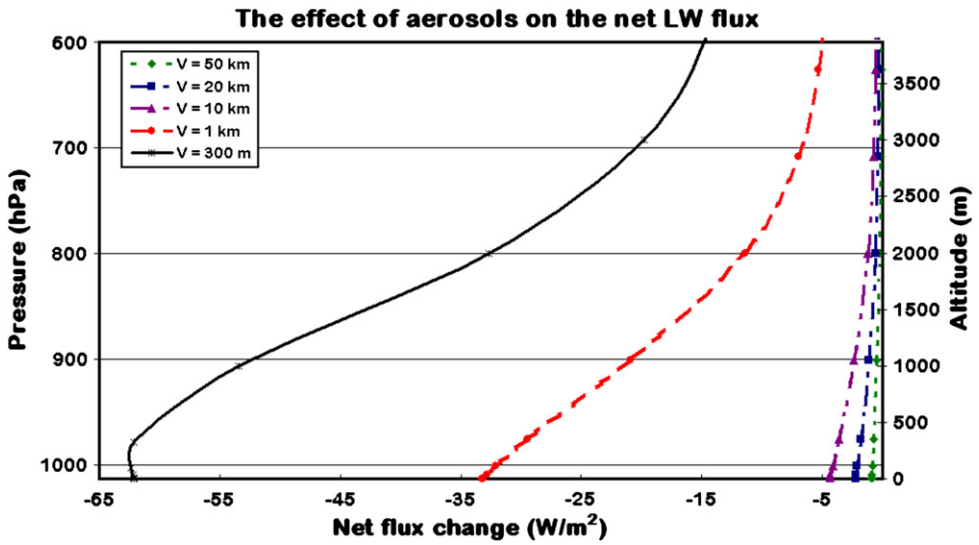

Fig. 7. The effect of aerosols on the net LW flux of the MLS case. Aerosol load was assumed to decay exponentially with scale height H = 1 km.

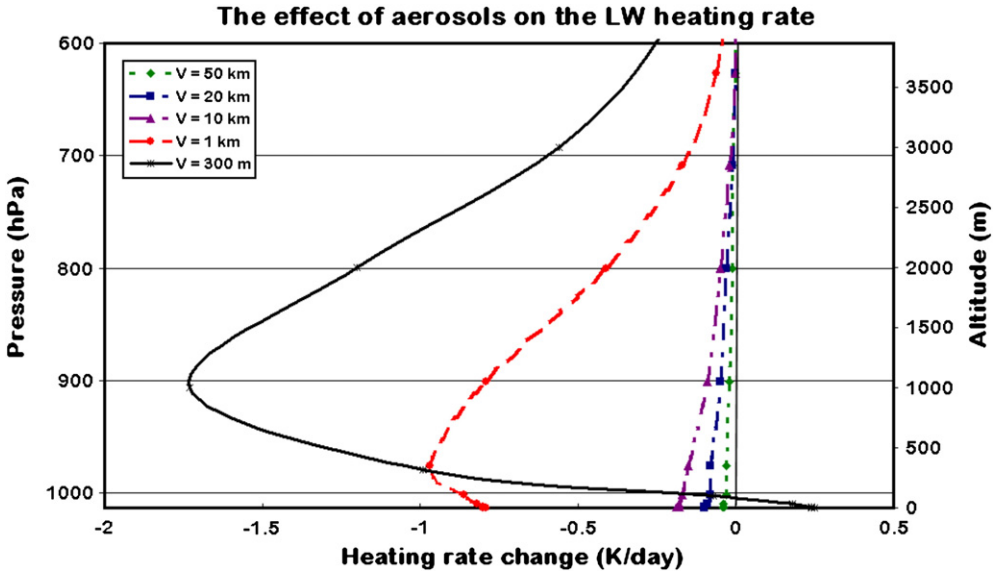

Fig. 8. The effect of aerosols on the LW heating rate of the MLS case. Aerosol load was assumed to decay exponentially with scale height H = 1 km.

clouds (Li and Fan, 2006). The greenhouse gases do not have such an indirect effect.

Acknowledgements

Professors T. Vesala and M. Kulmala, Dr. A. Lauri and M.Sc A. Lehtolainen, all from University of Helsinki, are acknowledged for providing advice and checking this article.

References

Claquin, T., Schulz, M., Balkanski, Y., 1997. A modeling study of the shortwave and longwave forcing by dust aerosols. J. Aerosol Sci. 28, 447–448.

Clough, S.A., Iacono, M.J., Moncet, J.L., 1992. Line-by-line calculations of atmospheric fluxes and cooling rates: application to water vapour. J. Geophys. Res. 97 (D14), 15761–15785.

Dammann, K.W., Hollmann, R., Stuhlmann, R., 2000. Study of aerosol impact on the earth radiation budget with satellite data. Adv. Space Res. 29, 1753–1757.

Deng, T., Zhang, L., Wu, D., Xia, J.L., Song, W., Deng, X.J., Tan, H.B., Bi, X.Y., Li, F., 2010. The high cloud and aerosol optical properties, as well as their radiative effects in Lan Zhou area. Plateau Meteorol. J. 29, 230–235.

Ellingson, R.G., Ellis, J., Fels, S.B., 1991. The intercomparison of radiation codes used in climate models: long wave results. J. Geophys. Res. 96 (D5), 8929–8953.

Han, Z., Li, J., Xia, X., Zhang, R., 2012. Investigation of direct radiative effects of aerosols in dust storm season over East Asia with an online coupled regional climate-chemistry-aerosol model. Atmos. Environ. 54, 688–699.

Hansell, R.A., Tsay, S.C., Ji, Q., Hsu, H.C., Jeong, M.J., Wang, S.H., Reid, J.S., Liou, K.N., Ou, S.C., 2010. An assessment of the surface longwave direct radiative effect of airborne Saharan dust during the NAMMA field campaign. J. Atmos. Sci. 67, 1048–1065.

Hartmann, D.L., 1994. Global Physical Climatology. Academic Press, New York.

Haywood, J.M., Allan, R.P., Culverwell, I., Slingo, T., Milton, S., Edwards, J., Clerbaux, N., 2005. Can desert dust explain the outgoing longwave

radiation anomaly over the Sahara during July 2003? J. Geophys. Res. 110, D05105.
Houghton, J.T., 2002. The physics of atmospheres, 3rd ed. Cambridge University Press, Cambridge.
Lenoble, J., 1986. Detection of stratospheric aerosol characteristics in relation with climate impact. Adv. Space Res. 6, 63–72.
Li, M., Fan, S.J., 2006. The progress of the climate effects of atmospheric aerosols research in China. Sci. Papers Online, China.
Method, T.J., Carlson, T.N., 1982. Radiative heating rates and some optical properties of the St. Louis aerosol, as inferred from aircraft measurements. Atmos. Environ. 16, 53–66.
Mickley, L.J., Leibensperger, E.M., Jacob, D.J., Rind, D., 2012. Regional warming from aerosol removal over the United States: Results from a transient 2010–2050 climate simulation. Atmos. Environ. 46, 545–553.
Paltridge, G.W., Platt, C.M.R., 1976. Radiative Processes in Meteorology and Climatology. Elsevier, Amsterdam.
Péré, J.C., Colette, A., Dubuisson, P., Bessagnet, B., Mallet, M., Pont, V., 2012. Impacts of future air pollution mitigation strategies on the aerosol direct radiative forcing over Europe. Atmos. Environ. 62, 451–460.
Ramachandran, S., Kedia, S., 2011. Aerosol radiative effects over an urban location and a remote site in western India: seasonal variability. Atmos. Environ. 45, 7415–7422.
Reck, R.A., 1974. Influence of surface albedo on the change in the atmospheric radiation balance due to aerosols. Atmos. Environ. 8, 823–833.
Reck, R.A., 1975. Influence of aerosol cloud height on the change in the atmospheric radiation balance due to aerosols. Atmos. Environ. 9, 89–99.
Roberts, R.E., Selby, J.A., Biberman, L.M., 1976. Infrared continuum absorption by atmospheric water vapour in the 8–12 μm window. Appl. Opt. 15, 2085–2090.
Savijärvi, H., 2006. Radiative and turbulent heating rates in the clear-air boundary layer. Q. J. R. Meteorol. Soc. 132, 147–161.
Savijärvi, H., Jin, L., 2001. Local winds in a valley city. Boundary-Layer Meteorol. 100, 301–319.
Shaocai, Y., Charles, S., Zender, S., Saxena, V.K., 2001. Direct radiative forcing and atmospheric absorption by boundary layer aerosols in the southeastern US: model estimates on the basis of new observations. Atmos. Environ. 35, 3967–3977.
Slingo, A., Ackerman, T.P., Allan, R.P., Kassianov, E.I., McFarlene, S.A., Robinson, G.J., Barnard, J.C., Miller, M.A., Harries, J.E., Russell, J.E., Dewitte, S., 2006. Observations of the impact of a major Saharan dust storm on the atmospheric radiation balance. Geophys. Res. Lett. 33, L24817.
Verma, S., Boucher, O., Upadhyaya, H.C., Sharma, O.P., 2006. Sulfate aerosols forcing: an estimate using a three-dimensional interactive chemistry scheme. Atmos. Environ. 40, 7953–7962.
Wendisch, M., Hellmuth, O., Ansmann, A., Heintzenberg, J., Engelmann, R., Althausen, D., Eichler, H., Müller, D., Hu, M., Zhang, Y., Mao, J., 2008. Radiative and dynamic effects of absorbing aerosol particles over the Pearl River Delta, China. Atmos. Environ. 42, 6405–6416.
Wu, B.Y., 1998. The Practical Algorithm of Atmospheric Radiative Transfer. Meteorological Press, China.
Zhang, H., Shen, Z., Wei, X., Zhang, M., Li, Z., 2012. Comparison of optical properties of nitrate and sulfate aerosol and the direct radiative forcing due to nitrate in China. Atmos. Res. 113, 113–125.
Zhao, X.J., Chen, C.H., Yuan, T., Zhang, W., Dong, X.J., 2005. The relationship between atmospheric aerosol optical thickness and its visibility in the winter of Lan Zhou city. Plateau Meteorol. J. 4, 617–622.

You Zhou is a Master's Degree student in the Division of Atmospheric Sciences of Department of Physics, University of Helsinki. Her nationality is Chinese. She obtained her Bachelor's Degree in Environmental Management in May 2010 from TAMK University of Applied Sciences in Tampere, Finland.

Hannu Savijärvi is a professor of meteorology in the Department of Physics, University of Helsinki. His studies have considered climate diagnostics, mesoscale modelling of various phenomena, cloud optics and radiative transfer, polar and boundary layer problems, and the dusty atmosphere of planet Mars.